A one-parameter model for turbine wakes from the entrainment hypothesis

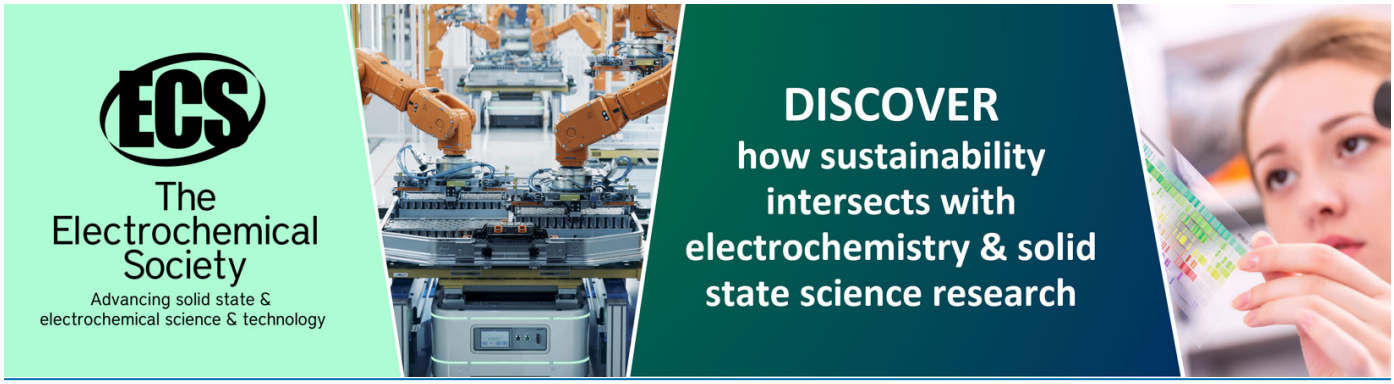

IOP Conf. Series: Journal of Physics: Conf. Series **1037** (2018) 072019 doi:10.1088/1742-6596/1037/7/072019

A one-parameter model for turbine wakes from the entrainment hypothesis

Paolo Luzzatto-Fegiz

Department of Mechanical Engineering, University of California, Santa Barbara, CA 93106, USA

E-mail: fegiz@engineering.ucsb.edu

Abstract. The entrainment hypothesis consists of a concise turbulence model, which has been widely used to model geophysical flows including plumes, gravity currents, and breaking internal waves. This paper employs the entrainment hypothesis to obtain a model for the wake of a single wind turbine, without having to linearize the governing equations, or needing to assume a wake radius that grows linearly (or in any other prescribed manner) with distance downstream. Assuming a top-hat velocity deficit and a zero pressure gradient, the analysis presented here re-discovers a result first due to Morton (B.R. Morton. *J. Fluid Mech.* 10:101–112, 1961), which however appears to have been completely overlooked until now. The predictions from this entrainment wake model are compared with published laboratory data and field observations, finding good agreement. Since the entrainment model does not require assuming a specific relationship between wake diameter and distance downstream, it may also enable simple extensions to account for complex terrain and for effects of yaw.

1. Introduction

Simple models for turbine wakes have been used extensively in the wind energy community, both as independent tools for engineering calculations, as well as to complement more refined and computationally-intensive techniques. One of the most popular approaches was introduced by Jensen [1], who developed a model assuming that the wake radius grows linearly with downstream distance x, and approximating the velocity deficit with a top-hat profile, as sketched in figure 1a. This model is often labeled the 'park' model; it is given by [1]

$$\frac{D_w(x)}{D} = \frac{D_i}{D} + 2k\frac{(x-x_i)}{D} \qquad \frac{U_w(x)}{U_o} = 1 - \frac{2a}{[1+2k(x-x_i)/D_i]^2}, \tag{1}$$

where U_w and U_o are the velocities inside and outside the wake, a is the axial induction coefficient (related to $C_t = 4a(1-a)$, such that $a = \frac{1}{2}\{1-\sqrt{1-C_t}\}$), D is the turbine diameter and D_i is the initial wake diameter, which starts at a downstream location x_i from the turbine. Following the approach of Frandsen [2], D_i is often set as the diameter after initial wake expansion, such that actuator disc theory gives $D_i = D[(1-a)/(1-2a)]^{1/2}$. The value of x_i is often set to zero [2]. The park model constitutes a pioneering and practically useful result, and has been widely implemented in the wind energy community [3, 4]. More recently, several authors [5, 6] noted that the park model does not conserve momentum. This fact can be verified by first

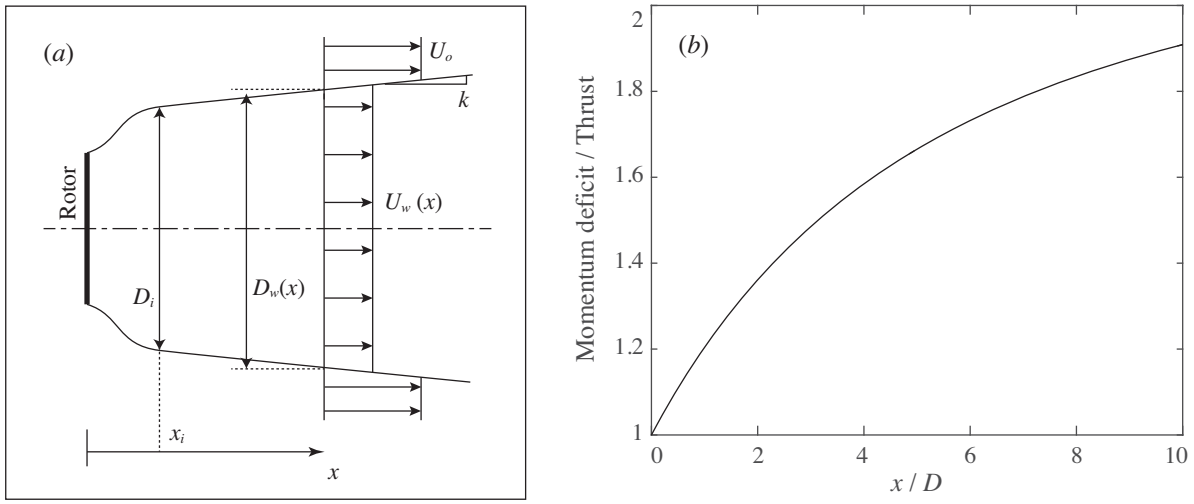

Figure 1. Park model. (a) Definition sketch (the initial wake expansion is exaggerated for clarity). (b) Wake momentum deficit, normalized by turbine thrust, for $C_t = 0.8$ and $k = 0.06$.

noting that, for a general axisymmetric wake with a top-hat profile, the x-momentum deficit (relative to a uniform stream U_o) is given by (e.g. [7])

$$\dot{M} = \rho \frac{\pi}{4} D_w^2 U_w (U_o - U_w), \tag{2}$$

where ρ is the density. Conservation of linear momentum implies that $\dot{M}$ should be constant and equal to the thrust on the turbine. If one evaluates $\dot{M}$ for the park model using (1), and differentiates it with respect to x, the result is

$$\frac{d\dot{M}_{park}}{dx} = \rho 4\pi a^2 k U_o^2 \frac{D_i^4}{[D_w(x)]^3} > 0, \tag{3}$$

such that $\dot{M}_{park}$ increases with x. The momentum deficit of the park model is plotted in figure 1b, using values of $C_t = 0.8$ and $k = 0.06$, which are typical in applications (values of k range between approximately 0.05 and 0.075 depending on terrain; see [6] and references therein). By $x/D = 10$, $\dot{M}_{park}$ has grown to approximately twice the thrust actually exerted by the turbine.

Frandsen *et al.* [5] proposed a momentum-conserving model, given by

$$\frac{D_w(x)}{D} = \frac{D_i}{D} + 2k^* \frac{(x - x_i)}{D} \qquad \frac{U_w(x)}{U_o} = \frac{1}{2}\left[1 + \sqrt{1 - \frac{8a(1-2a)}{[1 + 2k^*(x - x_i)/D_i]^2}}\right], \tag{4}$$

where the linear wake spreading parameter k^* is in general different from k. More recently, linear-spreading wake models that improve on the top-hat assumption have been introduced. These include FLORIS [8], which nests several linearly-spreading velocity deficit regions, as well as the model of Bastankhah & Porté-Agel [6], which employs a Gaussian velocity deficit. These models significantly improve agreement with experiments and Large Eddy Simulations of turbine wakes.

While the linear spreading assumption facilitates conceptual modeling, it requires empirical estimates of the spreading rate, which have not been related to more general turbulence parameterizations. In this paper, the assumption of a specific global relationship between D_w

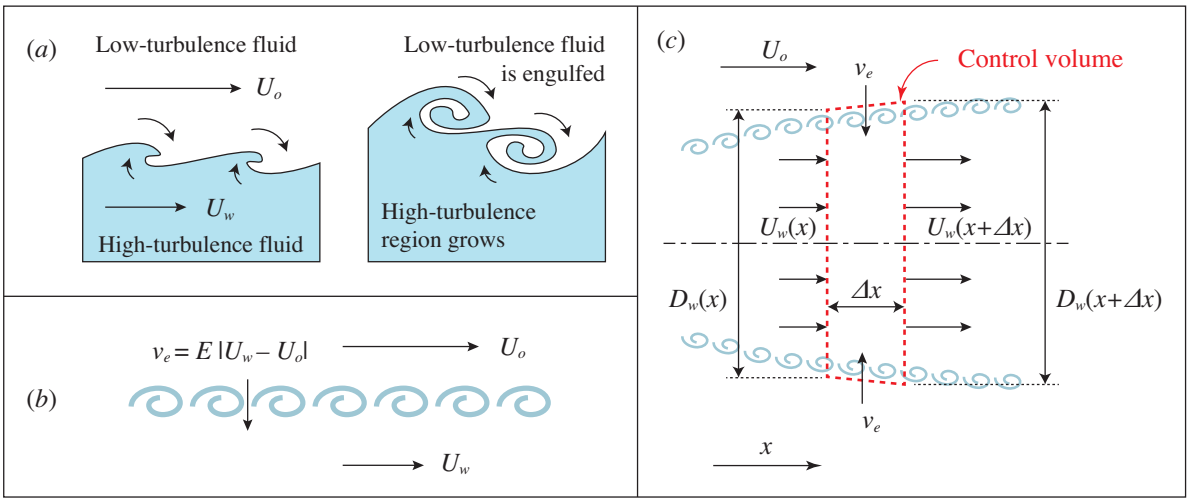

Figure 2. (a) Schematic illustration of growth of a high-turbulence region into relatively low-turbulence ambient fluid (after [16]). (b) Definition of the entrainment parameterization: low-turbulence fluid crosses the interface with velocity v_e. (c) Control volume used for mass and momentum budgets to derive the entrainment wake model.

and x is removed, by instead employing a simple, local turbulence closure that has seen wide usage in geophysical fluid dynamics, namely the entrainment hypothesis [9], which is outlined in section 2. In section 3, the entrainment hypothesis is used to obtain a model for wind turbine wakes. Section 4 compares the entrainment wake model to other approaches and to data for high Reynolds number wakes. Section 5 discusses the growth of the wake, its approximation by linear or other powers of x, as well as its asymptotic behavior. Concluding remarks follow in section 6.

2. The entrainment hypothesis

The 'entrainment hypothesis' consists of a simple turbulence parameterization, developed for flows where a strongly turbulent region advances into a relatively lower-turbulence background fluid. As noted earlier, this parameterization appears to have been first introduced by G.I. Taylor, in the context of modeling turbulent plumes [9]. This turbulence closure has had a vast impact on the environmental fluid dynamics literature; to date, reference [9] has accumulated 1,356 citations according to Web of Science. As previously mentioned, the entrainment hypothesis has been applied extensively in geophysical and industrial flow problems including plumes, jets, natural ventilation and gravity currents [9, 10, 11, 12, 13, 14, 15].

To describe this turbulence parameterization, consider an interface between a high-turbulence region and relatively low-turbulence ambient fluid, as sketched in figure 2a. Consistently with the definitions for a turbulent wake used so far in this paper, let the streamwise velocities in the high- and low-turbulence regions be U_w and U_o, respectively. The entrainment hypothesis assumes that fluid outside the turbulent region crosses the turbulent interface with an entrainment velocity of magnitude $v_e(x)$, which is proportional to the streamwise velocity difference across the interface, such that (see figure 2b)

$$v_e = E\,|U_o - U_w|\,, \tag{5}$$

where E is known as the entrainment coefficient (typically of the order of 0.1), which is obtained empirically [9]; see also section 4.

Similarly to the approach taken in the park and Frandsen models, here the axial velocity across the wake is approximated by a top-hat profile, such that U_o and U_w are the flow velocities

inside and outside the wake, and D_w defines the location of the wake boundary.

It has been observed that if E can be assumed to depend mainly on local processes, then its value should not change significantly even when one considers qualitatively different large-scale flows. Extensive oceanographic datasets exist to parameterize E as a function of local Reynolds number and Froude number (or, equivalently, Richardson number) ([14] and references therein). It is worth noting that these data were collected in field environments, where ambient turbulence is inevitably present. Introducing the entrainment hypothesis to turbine wake modeling could enable wind energy practitioners to leverage this wealth of established data on describing turbulent interfaces.

3. Entrainment model for wind turbine wakes

With reference to the wake sketched in figure 2*c*, consider a control volume of infinitesimal length Δx in the axial direction, whose diameter matches the diameter $D_w(x)$ of the wake. Assuming the fluid has uniform density, conservation of mass implies

$$\frac{\pi}{4}D_w^2U_w + v_e\pi D_w\Delta x = \frac{\pi}{4}D_w^2U_w + \frac{d}{dx}\left(\frac{\pi}{4}D_w^2U_w\right)\Delta x. \tag{6}$$

Dividing by $\pi\Delta x/4$, canceling the first term on each side, and re-arranging terms so the derivative is on the left-hand side,

$$\frac{d}{dx}\left(D_w^2U_w\right) = 4v_eD_w. \tag{7}$$

Using the definition of the entrainment velocity given by (5), and assuming $U_o > U_w$ to remove the absolute value,

$$\frac{d}{dx}\left(D_w^2U_w\right) = 4E(U_o - U_w)D_w. \tag{8}$$

In considering conservation of axial momentum, the pressure gradient is assumed to be negligible over the majority of the wake. This is typically the case after the wake has undergone the initial pressure adjustment shortly after the turbine. If the wake model is initialized after this initial pressure adjustment has already taken place, conservation of axial momentum yields

$$\frac{\pi}{4}D_w^2U_w^2 + v_e\pi D_w\Delta xU_o = \frac{\pi}{4}D_w^2U_w^2 + \frac{d}{dx}\left(\frac{\pi}{4}D_w^2U_w^2\right)\Delta x. \tag{9}$$

Similarly to the procedure used to obtain (8) from (6), the momentum equation (9) is divided by $\pi\Delta x/4$ and the first terms on each side cancel. Using the definition of v_e and moving the derivative to the left-hand-side, one obtains

$$\frac{d}{dx}\left(D_w^2U_w^2\right) = 4E(U_o - U_w)D_wU_o. \tag{10}$$

Equations (8) and (10) admit an analytical solution. Multiplying (8) by U_o and subtracting (10), the right-hand sides cancel out, leaving

$$U_o\frac{d}{dx}\left(D_w^2U_w\right) - \frac{d}{dx}\left(D_w^2U_w^2\right) = 0. \tag{11}$$

This can be integrated to give

$$D_w^2U_w(U_o - U_w) = C_1, \tag{12}$$

where C_1 is a constant. The left hand-side of (12) is the momentum deficit (2), divided by $\rho\frac{\pi}{4}$. Equation (12) therefore proves that the momentum deficit associated with the entrainment wake model is indeed constant. The value of C_1 can be found by requiring that the momentum deficit

must equate the thrust $T = C_t \frac{1}{2}\rho U_o^2 \frac{\pi}{4} D^2$, such that (12) becomes, after dividing both sides by $\rho U_o^2 \frac{\pi}{4} D^2$

$$\left(\frac{D_w}{D}\right)^2 \frac{U_w}{U_o}\left(\frac{U_o - U_w}{U_o}\right) = \frac{C_t}{2}. \tag{13}$$

Equation (13) can be used to eliminate D_w from the momentum equation (2), by first solving (13) for D_w

$$\frac{D_w}{D} = \left(\frac{C_t}{2}\right)^{1/2}\left[\frac{U_o}{U_w}\left(\frac{U_o}{U_o - U_w}\right)\right]^{1/2}. \tag{14}$$

Substituting (14) into (10) and simplifying,

$$\frac{d}{dx}\left(\frac{U_w}{U_o - U_w}\right) = \frac{4E}{D}\left(\frac{2}{C_t}\right)^{1/2}\left(\frac{U_o - U_w}{U_w}\right)^{1/2}. \tag{15}$$

Introducing the substitution

$$f = \frac{U_w}{U_o - U_w}, \tag{16}$$

equation (15) becomes

$$\frac{df}{dx} = \frac{4E}{D}\left(\frac{2}{C_t}\right)^{1/2} f^{-1/2}, \tag{17}$$

which can be integrated to give

$$\frac{2}{3} f^{3/2} = 4E\left(\frac{2}{C_t}\right)^{1/2}\frac{x}{D} + C_2 \equiv 4E\left(\frac{2}{C_t}\right)^{1/2}\left(\frac{x - x_v}{D}\right), \tag{18}$$

where the constant of integration C_2 has been re-written in terms of a 'virtual origin' x_v, which is a hypothetical location upstream where the wake would attain $U_w(x_v) = 0$. (This approach is common, for example, in models of plumes and jets [9].) To verify $U_w(x_v) = 0$, use the definition for f from (16) into (18), and multiply by 3/2

$$\left(\frac{U_w}{U_o - U_w}\right)^{3/2} = 6E\left(\frac{2}{C_t}\right)^{1/2}\frac{(x - x_v)}{D}. \tag{19}$$

To calculate the constant of integration x_v, use (18) and require that at a location x_i shortly downstream of the rotor (which is at $x = 0$) we have $U_w(x = x_i) = U_o(1 - 2a)$, consistently with actuator disc theory. The value of x_i may be selected from a model for wake expansion, or may be set to zero consistently with typical implementations of the park and Frandsen models. Therefore, setting $U_w(x = x_i) = U_o(1 - 2a)$ in (18) and solving for x_v,

$$\frac{x_v}{D} = \frac{x_i}{D} - \frac{(1 - 2a)^{3/2}(1 - a)^{1/2}}{12aE}. \tag{20}$$

To use C_t throughout the solution instead of a, employ $C_t = 4a(1 - a)$ to write $(1 - a) = C_t/(2a) - 1$, as well as $(1 - a) = C_t/(4a)$ and $a = \frac{1}{2}(1 - \sqrt{1 - C_t})$

$$\frac{x_v}{D} = \frac{x_i}{D} - \frac{(1 - C_t)^{3/4}(2C_t)^{1/2}}{12E\left[1 - (1 - C_t)^{1/2}\right]^{3/2}}. \tag{21}$$

For brevity, we define a rescaled x-variable

$$X = 6E\left(\frac{2}{C_t}\right)^{1/2}\frac{(x-x_v)}{D}, \tag{22}$$

$$= 6E\left(\frac{2}{C_t}\right)^{1/2}\frac{(x-x_i)}{D} + \frac{(1-C_t)^{3/4}}{[1-(1-C_t)^{1/2}]^{3/2}}, \tag{23}$$

such that solving (19) for U_w/U_o yields

$$\frac{U_w}{U_o} = \frac{X^{2/3}}{X^{2/3}+1}. \tag{24}$$

The wake diameter is found by substituting U_w/U_o from (24) into (14). After simplifying, and summarizing also the expressions for U_w and X, for convenience,

$$\frac{D_w}{D} = \left(\frac{C_t}{2}\right)^{1/2}\frac{X^{2/3}+1}{X^{1/3}}, \qquad \frac{U_w}{U_o} = \frac{X^{2/3}}{X^{2/3}+1},$$

$$X = 6E\left(\frac{2}{C_t}\right)^{1/2}\frac{(x-x_i)}{D} + \frac{(1-C_t)^{3/4}}{[1-(1-C_t)^{1/2}]^{3/2}}, \tag{25}$$

where, once again, x_i is the location where streamtube expansion associated with canonical actuator disc theory is assumed complete.

After obtaining (25) independently, the author found a paper of Morton [11], which provided the same result, through a different derivation, in the context of a broader discussion of entrainment models. Morton's paper appears to have been overlooked by the fluid dynamics and wind energy communities; according to Web of Science, it has accumulated only 16 citations over 57 years. The next section provides the first validation of this model.

4. Comparison to data and to other one-parameter wake models

To provide a consistent comparison between the three models, set $x_i = 0$ for all wake theories. As noted earlier, this practice is consistent with common implementations of the park model [2]. In order to test performance in realistic conditions, data is extracted from the literature, for field observations from full-scale turbines. To ensure a robust comparison between models and field data, $U(x,r,\theta)$ is averaged over the surface of a 'virtual' rotor at each x-location, as sketched in the inset of figure 3,

$$\langle U\rangle_{\rm rotor}(x) = \frac{4}{\pi D^2}\int_0^{2\pi}\int_0^{D/2} U(x,r,\theta)\, r\, dr\, d\theta. \tag{26}$$

The requirement that $U(x,r,\theta)$ be available over a transverse cross-section of the flow (rather than, say, only centerline measurements or velocity profiles) somewhat limits the data that can be used for this purpose. We employ field data collected by [17] (from their figure 5) as well as by [18] (based on power reduction between their turbines T41 and T42). The turbine-scale Reynolds number $Re = U_o D/\nu$ (with ν the kinematic viscosity) is approximately 6×10^7. In addition, the laboratory results of [18] are added, which have $Re \simeq 2\times10^4$ (specifically from their figure 7, which reports U over a transverse cross section at $x = 5D$).

The measurements above describe U in the wake. Since the flow of kinetic energy is proportional to $\langle U\rangle^3_{\rm rotor}$, the normalized wake power content $(\langle U\rangle_{\rm rotor}/U_o)^3$ is plotted versus x/D, shown by the symbols in figure 3. Each wake model is fitted with respect to their respective free parameter, finding the values $k = 0.067$, $k^* = 0.027$, $E = 0.15$.

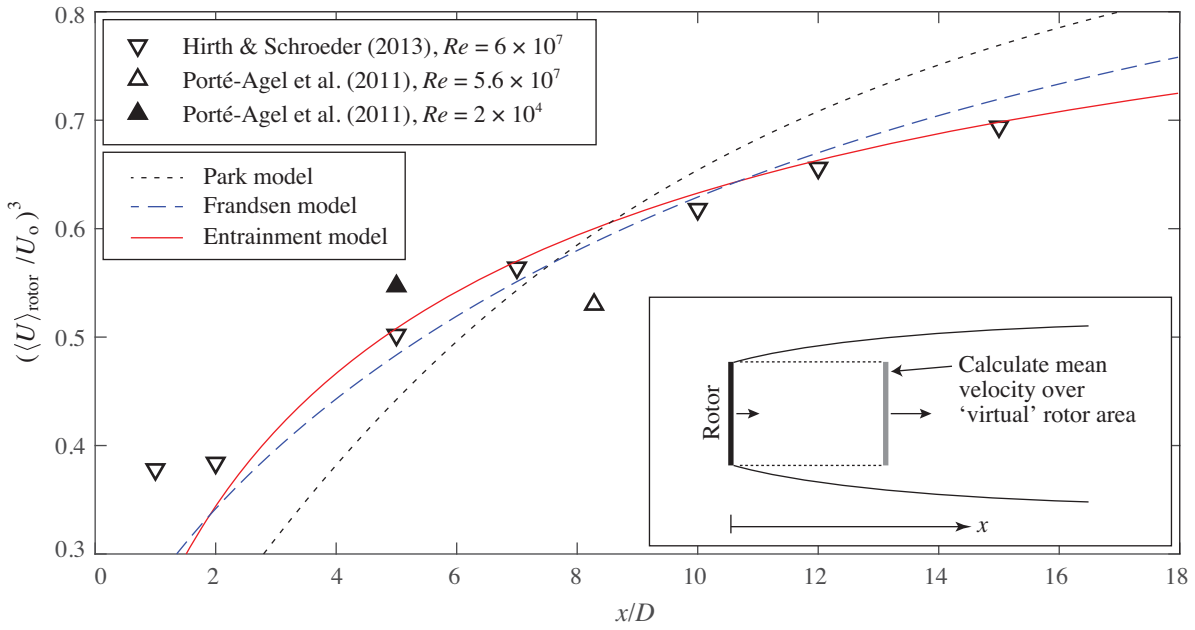

Figure 3. Power available in a turbine wake: comparison between one-parameter wake models (showing the original park model [1], the momentum-conserving model of reference [5], as well as the entrainment model) and data from field measurements [18, 17] and from laboratory experiments [18]. Each model has been fitted with respect to one parameter, which determines the spreading rate, yielding $k = 0.067$, $k^* = 0.027$ and $E = 0.15$.

5. Discussion: linearization, asymptotic behavior, and relation between k and E

It is interesting to examine the trends exhibited by the entrainment model in the light of the literature on axisymmetric turbulent wakes. Uberoi & Freymuth [19] examined the wake of a sphere at $Re \sim 8,600$, where they observed self-similarity for $x/D \gtrsim 50$, with $D_w \sim x^{1/3}$, consistently with canonical theory for turbulent axisymmetric wakes; this scaling was confirmed by subsequent experiments using discs and porous obstacles [7]. More recently, Eames *et al.* [20] proposed that wakes developing with a strongly turbulent inflow will scale as $D_w \sim x$. This scaling was supported by sphere wake data from [21] for $x/D \lesssim 6$, with $220 \lesssim Re \lesssim 1,100$ and turbulence intensity between 15% and 26%. Subsequently, [22] proposed that the $D_w \sim x$ scaling should also hold in wind turbine wakes. They presented experimental measurements behind a porous obstacle for $1 \lesssim x/D \lesssim 8$, at $Re \sim 34,000$ and with turbulence intensity of 18%. Rind & Castro [23] noted that the experiments supporting $D_w \sim x$ were performed for x/D values smaller than traditionally considered 'far wake' behavior in the free shear flow literature. In [23], they performed Direct Numerical Simulations (DNS, at $Re \sim 10,000$) with ambient turbulence between 2.2% and 8.7%, finding a scaling for D_w between $x^{1/3}$ and $x^{1/2}$, which was confirmed by subsequent DNS studies [24]. Nedić *et al.* [25] proposed that turbulent axisymmetric wakes behind complex objects could scale as $D_w \sim x^{1/2}$, due to the nonequilibrium scaling followed by the dissipation in the lee of such obstacles [26]. The scaling $D_w \sim x^{1/2}$ was supported by experiments at $Re \sim 80,000$, turbulence intensity around 5%, over the range $10 \lesssim x/D \lesssim 50$. In all of these studies, the turbulence lengthscale was of the order of the size of the obstacle.

In light of the findings of [20], and of the fact that several wake models assume a linearly-spreading wake [6], it is interesting to examine the result of linearizing the wake expansion in the entrainment model (25). Setting $x_i = 0$, noting D_w has no singularities for $x > 0$, a Taylor

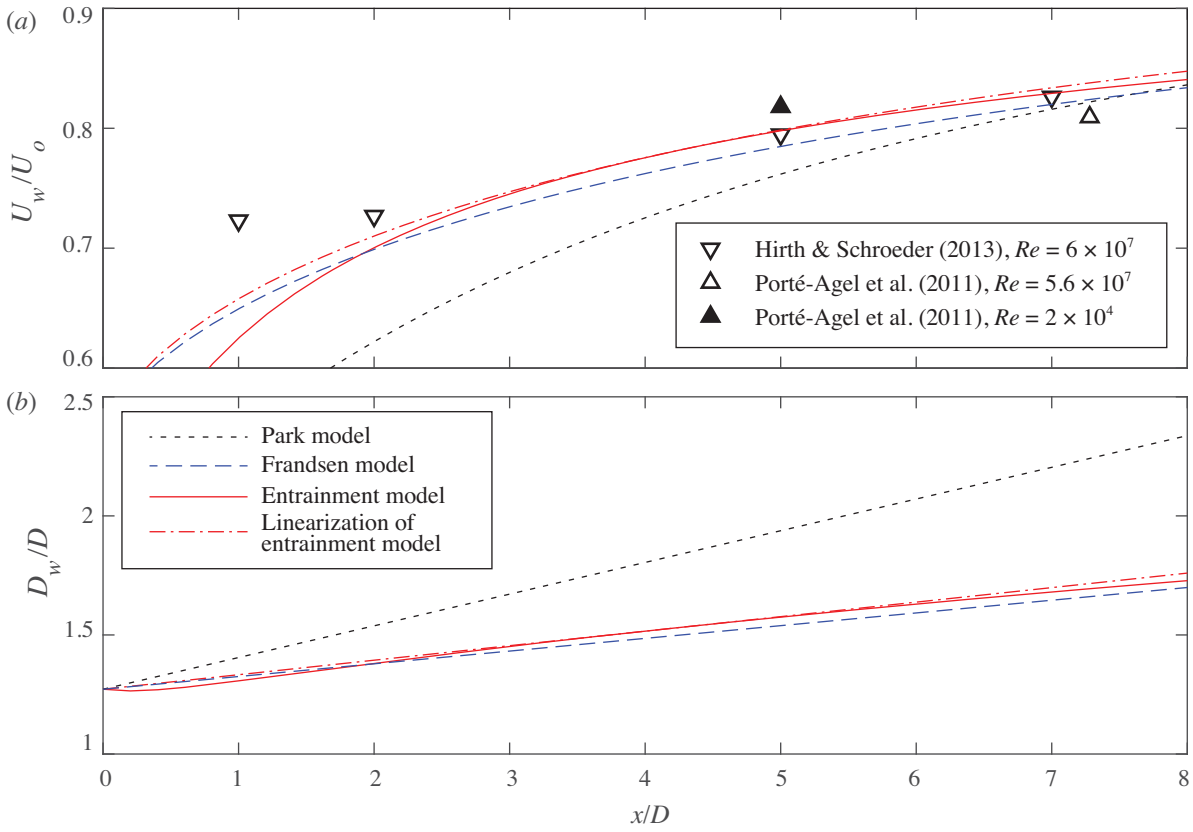

Figure 4. (a) Wake velocity U_w and (b) wake diameter D_w from the models considered in this paper, for $0 < x/D < 8$. The models, data and parameters match those in figure 3, with the addition of a linearization of the entrainment model (shown by the dot-dashed red line), showing that in this region the entrainment model is consistent with the scaling $D_w \sim x$.

expansion about a point $x_r > 0$ yields

$$\frac{D_w}{D} = \left(\left(\frac{C_t}{2}\right)^{\frac{1}{2}} \frac{\zeta^{2/3}+1}{\zeta^{1/3}} - 2E\frac{x_r}{D}\frac{\zeta^{2/3}-1}{\zeta^{4/3}}\right) + 2E\frac{\zeta^{2/3}-1}{\zeta^{4/3}}\frac{x}{D} + \mathcal{O}\left(\frac{(x-x_R)^2}{D^2}\right), \quad (27)$$

$$\zeta = 6E\left(\frac{2}{C_t}\right)^{\frac{1}{2}}\frac{x_r}{D} + \frac{(1-C_t)^{3/4}}{[1-(1-C_t)^{1/2}]^{3/2}}. \quad (28)$$

Define $D_{w,lin}$ as the linearly-spreading wake that results from neglecting the higher-order terms in (27). To choose a value of x_r, require that the first term on the right-hand side of (27) must equal the initial wake diameter $D_i/D = \sqrt{(1-a)/(1-2a)}$. This sets $x_r = x_{lin}$. Then

$$\frac{D_{w,lin}}{D} = \frac{D_i}{D} + 2k_E\frac{x}{D}, \quad \text{where} \quad k_E = E\frac{\zeta^{2/3}-1}{\zeta^{4/3}}, \quad (29)$$

where x_{lin} is found by solving (note that ζ also depends on x_{lin}, according to (28))

$$\left(\frac{C_t}{2}\right)^{\frac{1}{2}}\frac{\zeta^{2/3}+1}{\zeta^{1/3}} - 2Ex_{lin}\frac{\zeta^{2/3}-1}{\zeta^{4/3}} = \frac{D_i}{D}. \quad (30)$$

Equation (30) is solved numerically for various values of E and C_t. For $C_t = 0.8$ and $E = 0.15$, this yields $k_E = 0.031$, which is close to $k^* = 0.027$ found in section 4. The fact that k_E is weakly dependent on C_t is consistent with published data on turbulent wakes [7, 20, 25]. This relation between k_E and E enables relating the spreading parameter from the Frandsen model to a more general turbulence parameterization.

The value of $U_{w,lin}$ is found from $D_{w,lin}$ using momentum conservation (13). Figure 4 compares U_w and D_w from all models considered so far, for the range $0 < x/D < 8$ (as considered by [22]). The entrainment model is consistent with the linear wake scaling in this region.

Since the term 'far wake' has been used to imply widely different x/D ranges, the limit $x/D \to \infty$ here is denoted as the 'asymptotic wake'. The entrainment model exhibits canonical scalings

$$\lim_{x/D\to\infty} \frac{D_w}{D} = \left(\frac{C_t}{2}\right)^{1/2} X^{1/3}, \quad \lim_{x/D\to\infty} \frac{U_w}{U_o} = 1 - X^{-2/3}. \tag{31}$$

For the full solution (25) for D_w to be within 5% of the asymptotic prediction (31), one needs $x/D \gtrsim 55$ (with $C_t = 0.8$ and $E = 0.15$), implying that this asymptotic scaling emerges at very large x/D. Overall, it is not the purpose of this paper to make an argument for the applicability of one asymptotic wake scaling over another, for wind turbine wakes. For wind energy purposes, it is possible that concerns about asymptotic wake limits may be largely academic, and that the choice of a wind turbine wake model over another may ultimately be reasonably guided by ease of use and agreement with data.

6. Outlook

This paper shows that the entrainment hypothesis yields an axisymmetric wake model, which does not assume a globally valid relation between wake diameter and downstream distance. The entrainment wake model has an analytical solution, which is in good agreement with field measurements. The derivation shown here assumes the coefficient E does not change with x. This is consistent with the typical assumption, in the park and Frandsen wake models, that k and k^* are independent of x. It is in principle possible to let E depend on x, integrating (8) and (10) numerically, albeit at the cost of additional complexity.

Often k and k^* are assumed to depend on ambient turbulence levels or effective roughness z_0 of the terrain, and empirical parameterizations have been constructed to express this dependence [6]. One can seek similar parameterizations for E. It is worthwhile noting that in section 4 we found $E = 0.15$ according to field measurements, corresponding to a situation with high-Re and finite ambient turbulence. The value $E = 0.15$ therefore is likely to be close to an upper bound. Interestingly, measurements of entrainment in gravity currents and canopies also find that E is at most approximately 0.15 [14, 27]. Laboratory experiments may expect smaller Es, especially in cases involving laminar inflow or stable stratification. It may be interesting to use wind turbine wake data to systematically test, and possibly refine, existing parameterizations for E from geophysical fluid dynamics.

It is worthwhile noting that it is, in principle, possible to retain pressure gradient terms in the derivation of the momentum equation. The resulting set of governing equations may not admit an analytical solution, but may be integrated numerically, potentially enabling modeling wakes over complex terrain. It would also be valuable to introduce an equation for lateral momentum, as this may enable considering wake evolution behind a yawed rotor.

Acknowledgments

This work was partially supported by Churchill College, Cambridge through a Junior Research Fellowship, as well as by a Faculty Research Grant from the Academic Senate of the University of California, Santa Barbara. The author gratefully acknowledges interesting conversations on

the subject of entrainment with C.P. Caulfield and C. Cenedese, and thanks P. Rajborirug, N. Rommelfanger and one anonymous referee for helpful comments.

References

[1] I. Katic, J. Højstrup, and N. O. Jensen. A simple model for cluster efficiency. In *Proceedings of the European Wind Energy Association Conference and Exhibition*, pages 407–410, Rome, Italy, 1986.
[2] S. Frandsen. On the wind speed reduction in the center of large clusters of wind turbines. *J. Wind Eng. Ind. Aerodyn.*, 39(1-3):251–265, 1992.
[3] GH Windfarmer theory manual. Technical report, Garrad Hassan and Partners Ltd, 2009.
[4] Openwind theoretical basis and validation. Technical report, AWS Truepower, LCC, 2010.
[5] R. Frandsen, S. ad Barthelmie, S. Pryor, O. Rathmann, S. Larsen, J. Højstrup, and M. Thøgersen. Analytical modelling of wind speed deficit in large offshore wind farms. *Wind Energy*, 9:39–53, 2006.
[6] M. Bastankhah and F. Porté-Agel. A new analytical model for wind-turbine wakes. *Renewable Energy*, 70(C):116–123, 2014.
[7] S. B. Pope. *Turbulent Flows*. Cambridge University Press, 2000.
[8] P. M. O. Gebraad, F. W. Teeuwisse, J. W. van Wingerden, P. A. Fleming, S. D. Ruben, J. R. Marden, and L. Y. Pao. Wind plant power optimization through yaw control using a parametric model for wake effects-a CFD simulation study. *Wind Energy*, 19(1):95–114, 2014.
[9] B. R. Morton, G. Taylor, and J. S. Turner. Turbulent gravitational convection from maintained and instantaneous sources. *Proc. Roy. Soc. A*, 234:1–23, 1956.
[10] T. H. Ellison and J. S. Turner. Turbulent entrainment in stratified flows. *J. Fluid Mech.*, 6:423–448, 1959.
[11] B. R. Morton. On a momentum-mass flux diagram for turbulent jets, plumes and wakes. *J. Fluid Mech.*, 10:101–112, 1961.
[12] M. Princevac, H. J. S. Fernando, and C. D. Whiteman. Turbulent entrainment into natural gravity-driven flows. *J. Fluid Mech.*, 533:259–268, 2005.
[13] M. M. Scase and S. B. Dalziel. Internal wave fields generated by a translating body in a stratified fluid: an experimental comparison. *J. Fluid Mech.*, 564:305–331, 2006.
[14] C. Cenedese and C. Adduce. A new parameterization for entrainment in overflows. *J. Phys. Oceanogr.*, 40:1835–1850, 2010.
[15] I. A. Coomaraswamy and C. P. Caulfield. Time-dependent ventilation flows driven by opposing wind and buoyancy. *J. Fluid Mech.*, 672:33–59, 2011.
[16] G. M. Corcos and S. J. Lin. The mixing layer: deterministic models of a turbulent flow. Part 2. The origin of the three-dimensional motion. *J. Fluid Mech.*, 139:67–95, 1984.
[17] B. D. Hirth and J. L. Schroeder. Documenting wind speed and power deficits behind a utility-scale wind turbine. *J. Appl. Met. Climat.*, 52(1):39–46, 2013.
[18] F. Porté-Agel, Y.-T. Wu, H. Lu, and R. J. Conzemius. Large-eddy simulation of atmospheric boundary layer flow through wind turbines and wind farms. *J. Wind Eng. Ind. Aerod.*, 99(4):154–168, 2011.
[19] M. S Uberoi and P. Freymuth. Turbulent energy balance and spectra of the axisymmetric wake. *Phys. Fluids*, 13(9):2205–2210, 1970.
[20] I. Eames, P. B. Johnson, V. Roig, and F. Risso. Effect of turbulence on the downstream velocity deficit of a rigid sphere. *Phys. Fluids*, 23(9):095103, 2011.
[21] Z. Amoura, V. Roig, F. Risso, and A. Billet. Attenuation of the wake of a sphere in an intense incident turbulence with large length scales. *Phys. Fluids*, 22(5):055105, 2010.
[22] P. B. Johnson, C. Johnsson, S. Achilleos, and I. Eames. On the spread and decay of wind turbine wakes in ambient turbulence. *J. Phys.: Conf. Ser.*, 555:012055, 2014.
[23] E. Rind and I. P. Castro. Direct numerical simulation of axisymmetric wakes embedded in turbulence. *J. Fluid Mech.*, 710:482–504, 2012.
[24] A. Pal and S. Sarkar. Effect of external turbulence on the evolution of a wake in stratified and unstratified environments. *J. Fluid Mech.*, 772:361–385, 2015.
[25] J. Nedić, J. C. Vassilicos, and B. Ganapathisubramani. Axisymmetric turbulent wakes with new nonequilibrium similarity scalings. *Phys. Rev. Lett.*, 111(14):144503, 2013.
[26] R. E. Seoud and J. C. Vassilicos. Dissipation and decay of fractal-generated turbulence. *Phys. Fluids*, 19(10):105108, 2007.
[27] P. Luzzatto-Fegiz and C. P Caulfield. An entrainment model for fully-developed wind farms: effects of atmospheric stability and an ideal limit for wind farm performance. *Phys. Rev. Fluids*. Under revision. Available as arXiv eprint 1703.06553.